# Simulation study of BESIII with stitched CMOS pixel detector using ACTS

Yi Liu[1] · Xiao-Cong Ai[1] ⬝ · Guang-Yan Xiao[2] · Ya-Xuan Li[3] · Ling-Hui Wu[4] · Liang-Liang Wang[4] · Jia-Ning Dong[5] ⬝ ·
Ming-Yi Dong[4,6] ⬝ · Qing-Lin Geng[5] · Min Luo[7] · Yan Niu[5] · An-Qing Wang[5] · Chen-Xu Wang[7] · Meng Wang[5] ·
Lei Zhang[2] · Liang Zhang[5] · Rui-Kai Zhang[7] · Yao Zhang[4] · Ming-Gang Zhao[3] · Yang Zhou[4]

## Abstract

The reconstruction of the tracks of charged particles with high precision is crucial for HEP experiments to achieve their
physics goals. The BESIII drift chamber, which is used as the tracking detector of the BESIII experiment, has suffered from
aging effects resulting in degraded tracking performance after operation for approximately 15 years. To preserve and enhance
the tracking performance of BESIII, one of the proposals is to add one layer of a thin cylindrical CMOS pixel sensor based
on state-of-the-art stitching technology between the beam pipe and the drift chamber. The improvement in the tracking per-
formance of BESIII with such an additional pixel detector compared to that with only the existing drift chamber was studied
using the modern common tracking software ACTS, which provides a set of detector-agnostic and highly performant tracking
algorithms that have demonstrated promising performance for a few high-energy physics and nuclear physics experiments.

**Keywords** BESIII tracking detector · CMOS pixel sensor · Track reconstruction · Common tracking software

✉ Xiao-Cong Ai
  xiaocongai@zzu.edu.cn

1 School of Physics and Microelectronics, Zhengzhou
  University, Zhengzhou 450001, China

2 School of Physics, Nanjing University, Nanjing 210093,
  China

3 School of Physics, Nankai University, Tianjin 300071, China

4 Institute of High Energy Physics, Chinese Academy
  of Sciences, 19B Yuquan Road, Shijingshan District,
  Beijing 100049, China

5 Research Center for Particle Science and Technology,
  Institute of Frontier and Interdisciplinary Science, Shandong
  University, Qingdao 266237, China

6 University of Chinese Academy of Sciences, 19A Yuquan
  Road, Shijingshan District, Beijing 100049, China

7 School of Information Science and Engineering, Harbin
  Institute of Technology, Weihai 264209, China

## 1 Introduction

The Beijing Spectrometer (BESIII) [1] at the Beijing Elec-
tron-Positron (BEPCII) Collider has been a great success in
producing promising physics results [2] in the $\tau$-charm sec-
tor since 2009. However, after operating for approximately
15 years, the detectors at BESIII have been subjected to
aging effects, which degrade their performance [3].

The tracking detector at BESIII is a multilayer drift
chamber (MDC), which provides measurements of the
momentum and position of the charged tracks and informa-
tion of energy loss in unit path length, i.e., $\mathrm{d}E/\mathrm{d}x$ [4], of the
charged tracks for par-
ticle identification. As shown in Ref. [3, 5], due to the beam-
induced background with a hit rate up to 2 kHz/cm$^2$, the gain
of the MDC cells in the first ten layers has shown an obvious
decrease, with a maximum decrease in approximately 39% for
the innermost layer cells in 2017. This further reduces the spa-
tial and momentum resolution of the charged tracks. Because
BESIII is not expected to complete its mission in the foreseen
years [2, 3], the track reconstruction performance must be
preserved and enhanced to avoid compromising the physics
goals of BESIII, along with a possible upgrade of the tracking
system with state-of-the-art technologies for the detection of
charged particles. To obtain good preparation for the potential
malfunction of the MDC owing to the aforementioned aging

problem, plans to upgrade the BESIII inner tracker based on different technologies have been proposed [3]. This includes the replacement of the inner tracker with a new inner drift chamber [6] or a cylindrical gas electron multiplier (CGEM) tracker [7], which has attractive features such as high counting rate tolerance and low sensitivity to aging.

Compared with gaseous detectors, silicon pixel detectors have excellent spatial resolution and good radiation resistance. Therefore, an additional option for the BESIII inner-tracker upgrade is to use a large-area thin complementary metal oxide semiconductor (CMOS) pixel sensor with good spatial resolution based on cutting-edge stitching technology, which has already been used to produce CMOS pixel sensors for medical imaging applications [8–10]. The design for a first wafer-scale stitched sensor prototype, known as the monolithic stitched sensor (MOSS) chip, is discussed in recent studies. These efforts aim to enhance the performance of the vertex detector, i.e., the ITS3, at the ALICE experiment, as detailed in Ref. [11].

A Common Tracking Software (ACTS) [12] is a common high-energy physics (HEP) software. It provides a set of detector-agnostic, high-performance, and modular tools for the track reconstruction in HEP. The software leverages modern software technologies to facilitate concurrency, usability, maintenance, and extendability, addressing the prospective tracking challenges in HEP. To date, ACTS has been used for track reconstruction at ATLAS [13], FASER [14], sPHENIX [15], and STCF [16] for different types of tracking detectors. In particular, the promising tracking performance of ACTS for a tracking system with a drift chamber was first presented in Ref. [16].

In this study, the tracking performance of the BESIII MDC with an additional one-layer stitched cylindrical CMOS pixel detector inserted between the beam pipe and the inner wall of the MDC was studied using ACTS as the tracking software. The performance was compared with that of the current BESIII tracking detector using only the MDC based on the BESIII Offline Software System (BOSS) [17]. The remainder of this paper is organized as follows. In Sect. 2, the BESIII MDC and the proposed pixel detector based on the cylindrical CMOS pixel sensor are presented. Section 3 introduces the tracking strategies in BOSS and ACTS. The improvement in the tracking performance at BESIII with an additional pixel detector is presented in Sect. 4. Finally, a brief conclusion is provided in Sect. 5.

## 2 BESIII tracking detector and stitched CMOS pixel detector

The BESIII MDC is a cylindrical chamber operating with a helium-based gas mixture (He/$C_3H_8$ = 60:40) and is immersed in a 1-T magnetic field. The inner and outer radii of the MDC are 64 mm and 819 mm, respectively. The lengths of the wires range from 774 mm for the innermost layer to 2400 mm for the outermost layer. The drift cells, which are almost square-shaped, are arranged in 43 circular layers and alternate between the stereo layers and axial layers, i.e., in the order of eight stereo layers, 12 axial layers, 16 stereo layers, and 7 axial layers. The cell dimensions are approximately 12 mm × 12 mm for the eight inner layers and 16.2 mm × 16.2 mm for the 35 outer layers. The inner chamber is composed of 8 inner layers, and the outer chamber is composed of 35 outer layers.

CMOS pixel sensors have been widely used for vertex detectors in HEP because of their excellent spatial resolution down to a few $\mu m$, tolerance of high hit rates up to $10^8$ Hz/$cm^2$, and good detection efficiency and radiation resistance. For example, the CMOS pixel sensor has been used as the inner tracker or vertex detector at STAR experiments [18], ALICE experiments [19] and sPHENIX experiments [20]. It is also considered as the primary choice for pixel sensor technology in the CEPC physics program [21]. Despite the advantages of the CMOS pixel sensor, the tracking resolution of a traditional CMOS pixel detector, particularly for low-momentum tracks, can be limited by the irreducible material budget of the support structure and cooling pipe. This was demonstrated in Ref. [22], in which a MAPS-based CMOS pixel sensor was proposed to upgrade the BESIII inner chamber. Therefore, tracking based on traditional CMOS pixel sensors can be challenging at BESIII, in which tracks with a transverse momentum as low as 150 MeV must be reconstructed with good resolution.

In recent years, innovative stitching technologies have emerged with the aim of producing large-area sensors on one wafer, which can be further thinned to approximately 50 $\mu$m. With this thickness, the wafer can be curved into a cylindrical shape, thereby vastly simplifying the support structure and reducing the material budget. Based on this stitching technology, it is possible to construct a vertex detector using large-area thin CMOS pixel sensors with cylindrical shapes and simplified support structures. As discussed in Ref. [11], the material budget per pixel layer is expected to be reduced to 0.05% $X_0$ to allow bending of the silicon. In this study, we considered a vertex detector comprising a single layer of a stitched cylindrical pixel sensor with a thickness of 50 $\mu$m (0.05% $X_0$), as proposed in Ref. [11], length of 220 mm (including an insensitive area within 7 mm of each end), and a resolution of 8.66 $\mu$m and 57.74 $\mu$m in the r-$\phi$ and z directions, respectively. This layer was inserted between the 63-mm diameter beam pipe [1] and the MDC inner wall. The stitching technology foresees cooling by airflow and no readout circuits in the active area. Therefore, the additional material budget from the cooling and readout infrastructure, as well as the support structure in the active region of the pixel layer, is expected to have a negligible impact on the
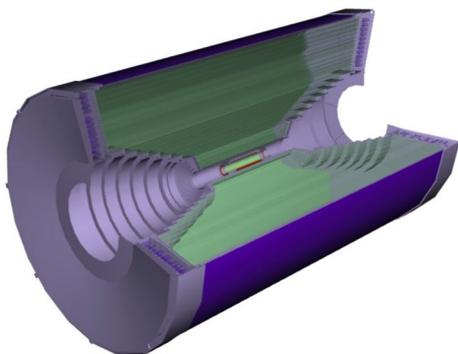
**Fig. 1** (Color online) Clipped view of the geometry of the BESIII MDC (cell wires are shown in green colors) and the pixel detector (shown in orange color) outside of the beampipe

tracking performance; hence, it was not considered in this study.

The geometry of the BESIII MDC and the pixel detector is shown in Fig. 1.

## 3 Tracking with BESIII offline software and ACTS

The simulation study was based on samples generated using BOSS, an offline software framework for event generation, simulation, reconstruction, performance validation, physics analysis, and visualization [23] for the BESIII experiment.

In BOSS, the production of both charmonium resonances and the continuum process from $e^+e^-$ collisions is provided by the KKMC [24] generator, and the decays of particles were modeled using EVTGEN [25], which can also be used to generate single-particle samples. The detector description is based on the Geometry Description Markup Language (GDML) [26], and the interaction of the particles with the detectors is simulated using GEANT4 [27].

The performance of the BESIII MDC with the additional pixel detector was studied using the ACTS software and compared with the performance of the BESIII MDC studied using the BESIII tracking software within BOSS. The workflow for studies of the tracking performance is illustrated in Fig. 2.

### 3.1 Tracking in BOSS

The trajectory of a charged particle in a magnetic field is parameterized using the helix track parameters at BESIII, as described in Ref. [28]. Track finding and track fitting are two tasks in BOSS track reconstruction. Track finding is a pattern-recognition problem of classifying measurements into subsets and creating track candidates, whereas track fitting is an estimation of the helix parameters. Two basic
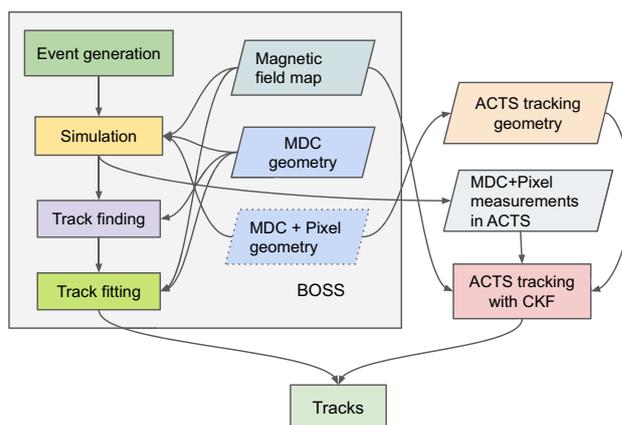


**Fig. 2** Workflow of tracking performance studies based on BOSS and ACTS

track-finding algorithms were implemented in BOSS: the template-matching algorithm (PAT) [29] and the track segment-finder algorithm (TSF) [28]. A specialized track-finding method called TCurlFinder [30] and a global track-finding method based on the Hough transform (HOUGH) [31] have been implemented to salvage low transverse momentum tracks with $p_T < 120$ MeV. In addition, an extended segment construction scheme that can achieve higher efficiency for low-transverse-momentum tracks has been developed [32]. The tracks found using these algorithms are combined and fed into a Kalman filter [33] for track fitting. Further track extrapolation is performed to obtain the track parameters of the other subdetectors at BESIII.

### 3.2 Tracking with ACTS

A detailed introduction to ACTS, including the geometry description, parameterization of the track parameters and measurements and tracking algorithms, can be found in Ref. [12]. The implementation of ACTS for track reconstruction of the BESIII tracking detector is outlined below.

To use ACTS for track reconstruction, the detector geometry with a detailed description of the detector material and placement, e.g., the GEANT4-based detector geometry, must be transformed into ACTS internal geometry, i.e., ACTS tracking geometry. This geometry has a simplified description of the passive detector material to facilitate fast navigation and track reconstruction. The TGEO [34] plugin in ACTS was used to transform the TGEO version of the BESIII detector geometry, which was created based on GDML exported from the GEANT4-based geometry, into the ACTS tracking geometry with material mapped to the auxiliary surfaces. The one pixel layer of the pixel detector was converted to a cylinder surface in ACTS and the 43 layers of signal wires of the MDC were converted to 43 layers of line surfaces, dedicated to

**Fig. 3** (Color online) Distributions of cosθ versus $p_T$ for $\mu$ (left) and $\pi$ (right) generated in $\psi(3686) \to \pi^+\pi^- J/\psi$, $J/\psi \to \mu^+\mu^-$ events
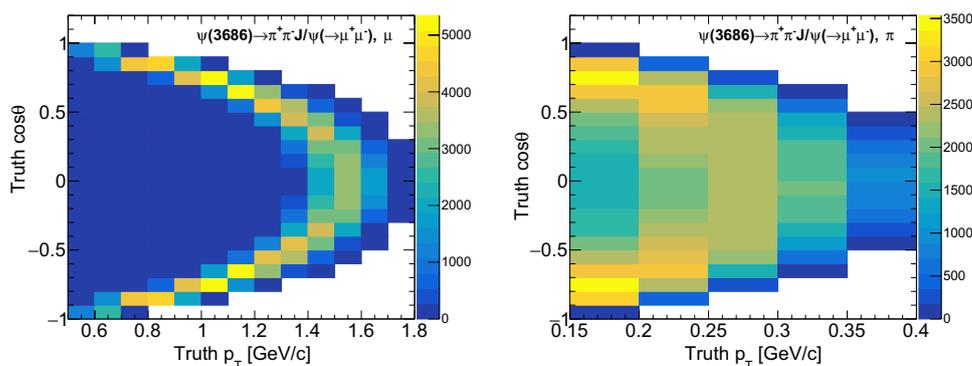
representation of measurements for a drift chamber or track parameters at the interaction point,[1] in ACTS.

The hits on the MDC after digitization were transformed into one-dimensional measurements associated with the line surfaces in ACTS, describing the drift distance of the drift chamber. The hits on the pixel detector after the simulation were transformed into two-dimensional measurements by smearing the simulated hits with the resolution of the pixel detector using Gaussian functions. These measurements are associated with ACTS cylinder surfaces, in which the local $x$ ($y$) coordinate represents $r \cdot \varphi$ ($z$) in the cylinder frame; that is, $r$ represents the radius of the cylinder, $\varphi$ represents the azimuthal angle of the position on the cylinder, and $z$ is the coordinate in the $z$ direction.

The BESIII magnetic field was transformed into an ACTS-interpolated magnetic field using the field map of the BESIII magnetic field. With an interpolated field provider in ACTS, the value of the magnetic field for any given position is calculated by interpolating from a grid of known values, e.g., eight corner points of a field cell in three-dimensional coordinate system.

Track fitting and finding are performed simultaneously using the combinatorial Kalman filter [35] algorithm in ACTS, which has the capability of rejecting noise hits based on the $\chi^2$ calculated using the distance between the hit and the predicted track parameters and the covariance of the hit and the predicted track parameters. If multiple hits are found to be compatible with the predicted track parameters, the hit with the best $\chi^2$ is used to filter out the track parameters. The smoothed track parameters from the first measurement are extrapolated to the beam line to obtain the estimated track parameters at the interaction point.

---

[1] Suppose the wire has a direction of **w** and the track direction is **t** in the global coordinate frame, the x axis and y axis in the local coordinate frame of a line surface is **w** × **t** and **w**, respectively.

# 4 Tracking performance studies

## 4.1 Monte-Carlo sample generation

The effect of the pixel detector on the resolution of the track parameters was studied using single $\mu^-$ and single $\pi^-$ samples. The samples were generated with a fixed transverse momentum $p_T$, cosθ (θ is the polar angle) uniformly distributed between [−0.8, 0.8], and an azimuthal angle $\phi$ uniformly distributed in the range of $[0, 2\pi]$. The impact of the pixel detector on the tracking efficiency was studied using $\psi(3686) \to \pi^+\pi^- J/\psi, J/\psi \to \mu^+\mu^-$ events generated at $\sqrt{s}$ = 3.686 GeV. The two-dimensional distributions of cosθ and $p_T$ for $\mu$ and $\pi$ during this process are shown in Fig. 3.

Random background hits in the MDC due to beam-related background or electronic noise were generated in the standard simulation sample production at BESIII. Because a dedicated background noise model for the pixel detector is not yet available, no background noise was considered for the inserted pixel layer in this study.

## 4.2 Track reconstruction performance

The resolution of the impact track parameters, $d_0$ and $z_0$, and the relative resolution of the transverse momentum $p_T$ as a function of $p_T$ for the BESIII MDC with an additional pixel layer, which is placed with radius $r_{pixel}$ at three different values (i.e., 35 mm, 45 mm, or 55 mm) compared to those of BESIII MDC, are shown in Fig. 4. Although $r_{pixel}$ has little impact on the resolution of $p_T$, the spatial resolution is better with a smaller $r_{pixel}$. With $r_{pixel}$ = 35 mm, the resolution of $d_0$ and $z_0$ is 60 $\mu$m and 120 $\mu$m for $\mu^-$ and $\pi^-$ with $p_T$ = 1 GeV, respectively, and the relative resolution of 44% for $p_T$ at $p_T$ = 1 GeV was achieved. The resolutions of $d_0$, $z_0$, $p_T$ can be improved by up to 67%, 93%, and 32%, respectively, by adding the proposed pixel detector to the current BESIII tracking detector.

A comparison of the tracking efficiency, which is defined as the fraction of the generated charged particles which have the corresponding reconstructed tracks in the detector region
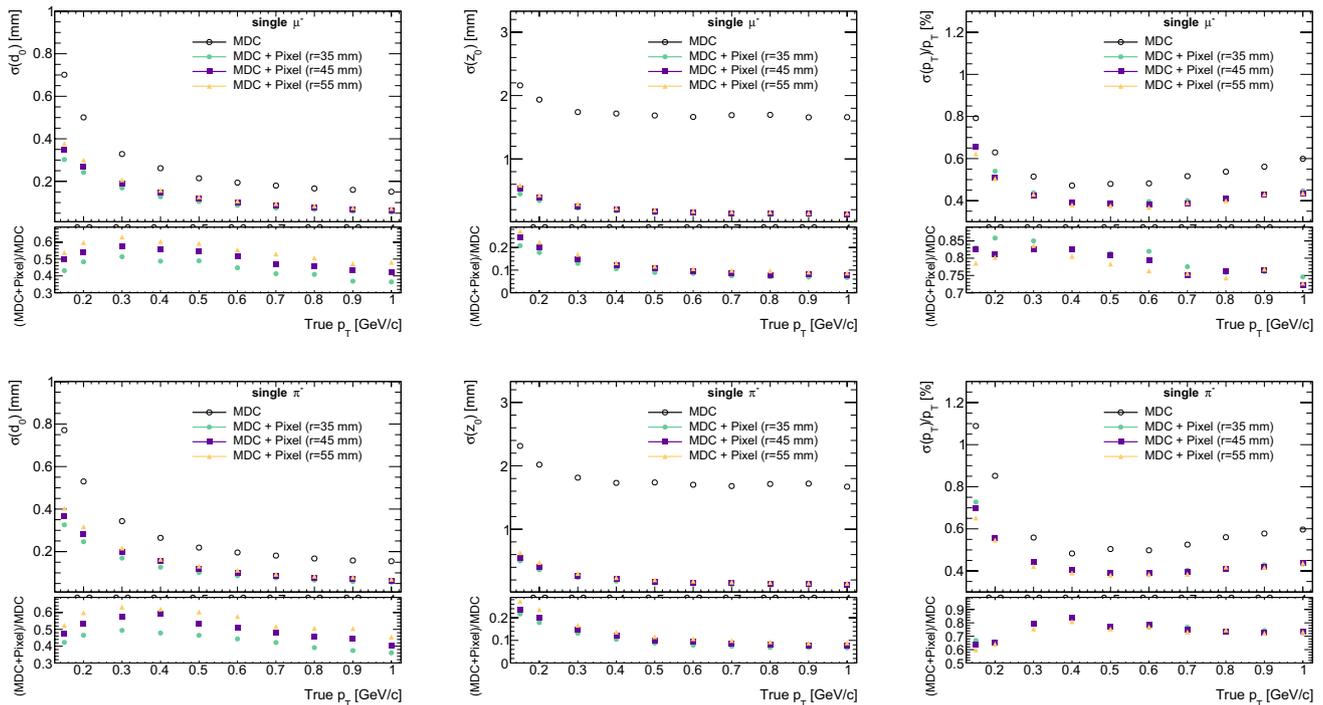
**Fig. 4** The resolution of $d_0$ (left), $z_0$ (middle) and relative resolution of $p_T$ (right) for single $\mu^-$ (top) and single $\pi^-$ (bottom) as a function of particle $p_T$ for the BESIII MDC only (black circle), and BESIII MDC with an additional pixel layer (denoted as "Pixel") placed with $r_{pixel} = 35$ mm (blue dot), 45 mm (purple triangle) and 55 mm (yellow triangle), respectively

($|\cos\theta| < 0.93$), between the BESIII MDC with the additional pixel layer and the BESIII MDC alone is shown in Fig. 5. The additional pixel layer can significantly improve the tracking efficiency for tracks with a particularly low momentum or large $|\cos\theta|$. For $\mu$ with $p_T$ below 0.6 GeV in the $\psi(3686) \rightarrow \pi^+\pi^- J/\psi, J/\psi \rightarrow \mu^+\mu^-$ process, the improvement can reach 9%. The improvement can reach 10% for $\pi$ with $0.85 < |\cos\theta| < 0.93$. A pixel with $r_{pixel} = 35$ mm provides better tracking efficiency than the other two choices.

# 5 Conclusion

After operating for approximately 15 years, the tracking detector of BESIII experiment has suffered from aging effects and must be upgraded to preserve its tracking performance for BESIII to fulfill its remaining physics goals in the next few years. The possibility of inserting a one-layer pixel detector using a large-area thin cylindrical CMOS pixel sensor based on stitching technology between the beam pipe and the MDC was considered. The spatial and momentum resolutions were studied using ACTS and compared with the performance of the current BESIII tracking detector obtained using the BESIII offline software. The proposed method based on the stitched cylindrical CMOS pixel sensor was found to be promising, i.e., the resolution of $d_0$, $z_0$, $p_T$ can be improved by up to 67%, 93%, and 32%, respectively, and the tracking efficiency for particles in the $\psi(3686) \rightarrow \pi^+\pi^- J/\psi, J/\psi \rightarrow \mu^+\mu^-$ events can be improved by up to 10% in the low $p_T$ or large $|\cos\theta|$ region, with the additional pixel layer placed at a radius of 35 mm. Meanwhile, this is the first time that ACTS has been used for track reconstruction for a drift chamber with calibrated measurements and realistic noise hits. In future studies, the noise model of this state-of-the-art pixel detector will be studied, and the tracking performance considering the noise of the pixel detector will be investigated.

**Fig. 5** The tracking efficiency of $\mu$ (top), $\pi$ (bottom) in the process of $\psi(3686) \rightarrow \pi^+\pi^- J/\psi, J/\psi \rightarrow \mu^+\mu^-$ as a function of particle $p_T$ (left) and $\cos\theta$ (right) for the BESIII MDC only (black circle), and BESIII MDC with an additional pixel layer (denoted as "Pixel") placed with $r_{pixel} = 35$ mm (blue dot), 45 mm (purple triangle) and 55 mm (yellow triangle), respectively
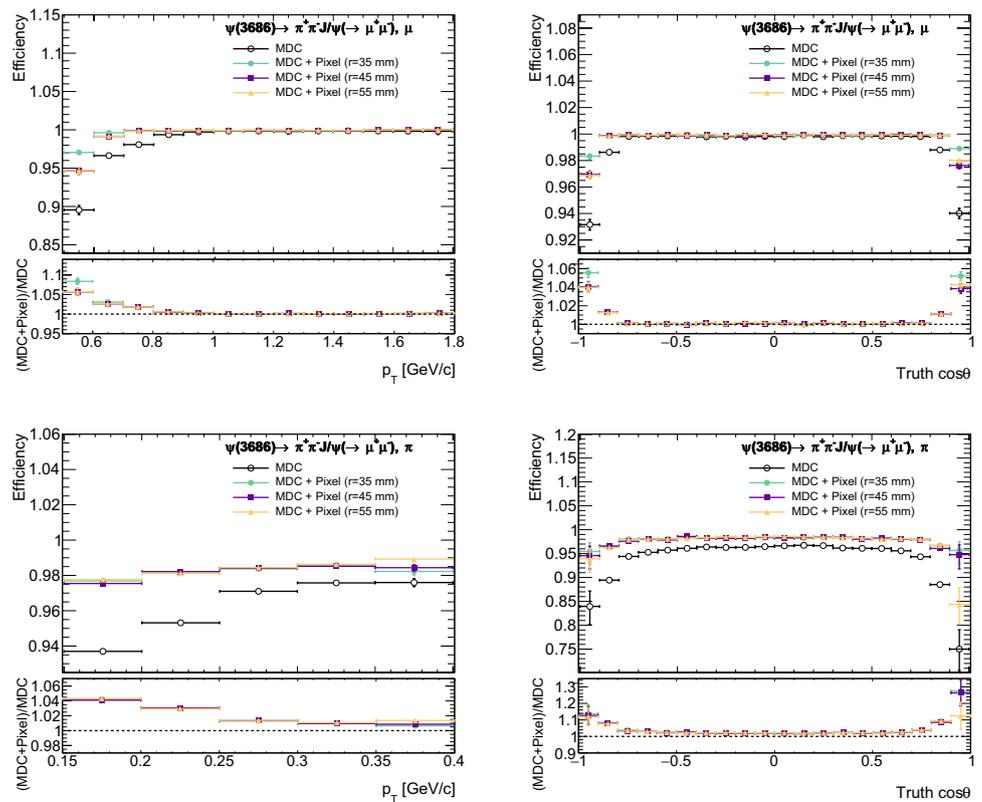
**Author Contributions** All authors contributed to the study conception and design and material preparation. The analysis was performed by Yi Liu, Guang-Yan Xiao and Ya-Xuan Li. The first draft of the manuscript was written by Xiao-Cong Ai and Ling-Hui Wu, and all authors commented on previous versions of the manuscript. All authors read and approved the final manuscript.

**Data availability** The data that support the findings of this study are openly available in Science Data Bank at https://www.doi.org/10.57760/sciencedb.13616 and https://cstr.cn/31253.11.sciencedb.13616.

## Declarations

**Conflict of interest** The authors declare that they have no competing interests.

## References

1. M. Ablikim, Z.H. An, J.Z. Bai et al., Design and construction of the BESIII detector. Nucl. Instrum. Meth. A **614**, 345–399 (2010). https://doi.org/10.1016/j.nima.2009.12.050
2. C.Z. Yuan, S.L. Olsen, The BESIII physics programme. Nat. Rev. Phys. **1**, 480–494 (2019). https://doi.org/10.1038/s42254-019-0082-y
3. M. Ablikim, M.N. Achasov, P. Adlarson et al., Future physics programme of BESIII *. Chin. Phys. C **44**, 040001 (2020). https://doi.org/10.1088/1674-1137/44/4/040001
4. X.X. Cao, W.D. Li, C.L. Liu et al., Studies of d$E$/d$x$ measurements with the BESIII. Chin. Phys. C **34**, 1852 (2010). https://doi.org/10.1088/1674-1137/34/12/012
5. M.Y. Dong, Q.L. Xiu, L.H. Wu et al., Aging effect in the BESIII drift chamber*. Chin. Phys. C **40**, 016001 (2016). https://doi.org/10.1088/1674-1137/40/1/016001
6. Y.J. Xie, Z.H. Qin, X.Y. Ma et al., Construction and cosmic-ray test of the new inner drift chamber for BESIII. Chin. Phys. C **40**, 096003 (2016). https://doi.org/10.1088/1674-1137/40/9/096003
7. A. Bortone, Development and operation of the CGEM Inner Tracker for the BESIII experiment. Nucl. Instrum. Meth. Phys. Res. Sect. A **1048**, 167957 (2023). https://doi.org/10.1016/j.nima.2022.167957
8. S. Bohndiek, A. Blue, J. Cabello et al., Characterization and testing of LAS: a prototype 'large area sensor' with performance characteristics suitable for medical imaging applications. IEEE Trans. Nucl. Sci. **56**, 2938–2946 (2009). https://doi.org/10.1109/TNS.2009.2029575
9. A. Konstantinidis, M. Szafraniec, R. Speller et al., The Dexela 2923 CMOS X-ray detector: a flat panel detector based on CMOS active pixel sensors for medical imaging applications. Nucl. Instrum. Meth. Phys. Res. Sect. A **689**, 12–21 (2012). https://doi.org/10.1016/j.nima.2012.06.024
10. M. Farrier, T. Achterkirchen, G. Weckler et al., Very large area CMOS active-pixel sensor for digital radiography. IEEE Trans. Electron Devices **56**, 2623–2631 (2009). https://doi.org/10.1109/TED.2009.2031001
11. G. Aglieri Rinella, Developments of stitched monolithic pixel sensors towards the ALICE ITS3. Nucl. Instrum. Meth. Phys. Res. Sect. A **1049**, 168018 (2023). https://doi.org/10.1016/j.nima.2023.168018
12. X. Ai, C. Allaire, N. Calace et al., A common tracking software project. Comput. Softw. Big Sci. **6**, 8 (2022). https://doi.org/10.1007/s41781-021-00078-8
13. ATLAS Collaboration, Software Performance of the ATLAS Track Reconstruction for LHC Run 3. Tech. rep., CERN, Geneva,

all figures including auxiliary figures are available at https://atlas.web.cern.ch/Atlas/GROUPS/PHYSICS/PUBNOTES/ATL-PHYS-PUB-2021-012 (May 2021)

14. H. Abreu, J. Anders, C. Antel et al., First direct observation of collider neutrinos with FASER at the LHC. Phys. Rev. Lett. **131**, 031801 (2023). https://doi.org/10.1103/PhysRevLett.131.031801

15. J.D. Osborn, A.D. Frawley, J. Huang et al., Implementation of ACTS into sPHENIX track reconstruction. Comput. Softw. Big Sci. **5**, 23 (2021). https://doi.org/10.1007/s41781-021-00068-w

16. X. Ai, X. Huang, Y. Liu, Implementation of ACTS for STCF track reconstruction. J. Instrument. **18**, P07026 (2023). https://doi.org/10.1088/1748-0221/18/07/P07026

17. BESIII Offline Software System. https://bes3.readthedocs.io/index.html

18. A. Dorokhov, G. Bertolone, J. Baudot et al., High resistivity CMOS pixel sensors and their application to the STAR PXL detector. Nucl. Instrum. Meth. Phys. Res. Sect. A **650**, 174–177 (2011). https://doi.org/10.1016/j.nima.2010.12.112

19. G. Aglieri Rinella, The ALPIDE pixel sensor chip for the upgrade of the ALICE inner tracking system. Nucl. Instrum. Meth. Phys. Res. Sect. A **845**, 583–587 (2017). https://doi.org/10.1016/j.nima.2016.05.016

20. Y. Ji, sPHENIX Collaboration, Heavy flavor physics with the sphenix maps vertex tracker upgrade. Nucl. Phys. A **1005**, 121792 (2021). https://doi.org/10.1016/j.nuclphysa.2020.121792

21. S. Dong, P. Yang, Y. Zhang et al., Design and characterisation of the JadePix-3 CMOS pixel sensor. Nucl. Instrum. Meth. Phys. Res. Sect. A **1048**, 167967 (2023). https://doi.org/10.1016/j.nima.2022.167967

22. M. Dong, X. Ju, X. Tian et al., Development of maps-based detector ladders for the besiii inner tracker upgrade. Nucl. Instrum. Meth. Phys. Res. Sect. A **924**, 287–292 (2019).https://doi.org/10.1016/j.nima.2018.06.032

23. K.X. Huang, Z.J. Li, Z. Qian et al., Method for detector description transformation to unity and application in besiii. Nucl. Sci. Tech. **33**, 142 (2022). https://doi.org/10.1007/s41365-022-01133-8

24. S. Jadach, B.F.L. Ward, Z. Was, Coherent exclusive exponentiation for precision Monte Carlo calculations. Phys. Rev. D **63**, 113009 (2001). https://doi.org/10.1103/PhysRevD.63.113009

25. D.J. Lange, The EvtGen particle decay simulation package. Nucl. Instrum. Meth. A **462**, 152–155 (2001). BEAUTY2000, Proceedings of the 7th International Conference on B-Physics at Hadron Machines. https://doi.org/10.1016/S0168-9002(01)00089-4

26. Geometry Description Markup Language (GDML)., https://gdml.web.cern.ch/GDML

27. S. Agostinelli, J. Allison, K. Amako et al., Geant4-a simulation toolkit. Nucl. Instrum. Meth. Phys. Res. Sect. A **506**, 250–303 (2003). https://doi.org/10.1016/S0168-9002(03)01368-8

28. Q.G. Liu, S.L. Zang, W.G. Li et al., Track reconstruction using the TSF method for the BESIII main drift chamber. Chin. Phys. C **32**, 565 (2008). https://doi.org/10.1088/1674-1137/32/7/011

29. Y. Zhang, X.Y. Zhang, W.D. Li et al., Pattern-matching track reconstruction for the BESIII main drift chamber. High Energy Phys. Nucl. Phys. **31**, 570–575 (2007)

30. L.K. Jia, Z.P. Mao, W.D. Li et al., Study of low momentum track reconstruction for the BESIII main drift chamber. Chin. Phys. C **34**, 1866 (2010). https://doi.org/10.1088/1674-1137/34/12/014

31. J. Zhang, Y. Zhang, H.M. Liu et al., Low transversemomentum track reconstruction based on the Hough transform for the BESIII drift chamber. Radiation Detect. Technol. Methods **2**, 20 (2018). https://doi.org/10.1007/s41605-018-0052-4

32. C.L. Ma, Y. Zhang, Y. Yuan et al., An extended segment pattern dictionary for a pattern matching tracking algorithm at BESIII. Chin. Phys. C **37**, 066202 (2013). https://doi.org/10.1088/1674-1137/37/6/066202

33. J.K. Wang, Z.P. Mao, J.M. Bian et al., BESIII track fitting algorithm. Chin. Phys. C **33**, 870 (2009). https://doi.org/10.1088/1674-1137/33/10/010

34. R. Brun, A. Gheata, M. Gheata, The ROOT geometry package. Nucl. Instrum. Methods. Phys. Res. A **502**, 676–680 (2003). https://doi.org/10.1016/S0168-9002(03)00541-2

35. R. Frühwirth, A. Strandlie, Track Finding, (Springer International Publishing, Cham, 2021), pp. 81–102. https://doi.org/10.1007/978-3-030-65771-0_5